Development 133, 1069-1077 (2006) doi:10.1242/dev.02281

Early Hedgehog signaling from neural to oral epithelium organizes anterior craniofacial development

Johann K. Eberhart*, Mary E. Swartz, Justin Gage Crump and Charles B. Kimmel

Hedgehog (Hh) signaling plays multiple roles in the development of the anterior craniofacial skeleton. We show that the earliest function of Hh is indirect, regulating development of the stomodeum, or oral ectoderm. A subset of post-migratory neural crest cells, that gives rise to the cartilages of the anterior neurocranium and the pterygoid process of the palatoquadrate in the upper jaw, condenses upon the upper or roof layer of the stomodeal ectoderm in the first pharyngeal arch. We observe that in mutants for the Hh co-receptor *smoothened* (*smo*) the condensation of this specific subset of crest cells fails, and expression of several genes is lost in the stomodeal ectoderm. Genetic mosaic analyses with *smo* mutants show that for the crest cells to condense the crucial target tissue receiving the Hh signal is the stomodeum, not the crest. Blocking signaling with cyclopamine reveals that the crucial stage, for both crest condensation and stomodeal marker expression, is at the end of gastrulation – some eight to ten hours before crest cells migrate to associate with the stomodeum. Two Hh genes, *shh* and *twhh*, are expressed in midline tissue at this stage, and we show using mosaics that for condensation and skeletogenesis only the ventral brain primordium, and not the prechordal plate, is an important Hh source. Thus, we propose that Hh signaling from the brain primordium is required for proper specification of the stomodeum and the stomodeum, in turn, promotes condensation of a subset of neural crest cells that will form the anterior neurocranial and upper jaw cartilage.

KEY WORDS: Hedgehog, Neurocranium, Neural Crest, Pharyngeal Arch, Stomodeum, Zebrafish

INTRODUCTION

Hedgehog (Hh) signaling is crucial for the development of the anterior face and skull. Loss of function of a key Hh molecule, Sonic hedgehog (Shh), causes a wide variety of craniofacial defects, and it is clear that Shh is involved in multiple steps of craniofacial development (Cordero et al., 2004). However, the existence of these multiple signaling events means that the precise roles of Hh signaling in individual steps remain largely unresolved.

Evidence that Hh plays a role in early craniofacial patterning comes from two different kinds of analyses. First, whereas complete loss of either Shh or the Hh co-receptor, Smoothened (Smo), causes nearly complete cartilage loss (Brand et al., 1996; Chen et al., 2001; Chiang et al., 1996; Hu and Helms, 1999; Roessler et al., 1996), less severe disruptions of the Hh pathway produce defects more specific to the anterior neurocranium (Brand et al., 1996). Second, targeted inactivation of *Smo* in the mouse, as well as functional studies in the chicken have shown that Hh signaling is required for the patterning and outgrowth of the precursors of the craniofacial skeleton (Abzhanov and Tabin, 2004; Hu et al., 2003; Jeong et al., 2004; Washington et al., 2005). These analyses suggest a model in which the precursor domain for the anterior craniofacial skeletal is especially sensitive to Hh disruption. Therefore, we have detailed the role that Hh plays in patterning the specific precursor domain of the anterior neurocranium.

Here, we show that zebrafish Hh pathway mutants lose a specific domain of neural crest-derived skeletal precursors, which normally condense on the superior surface, or roof, of the stomodeum. By fate mapping and time-lapse analyses, we find that the neural crest cell precursors for the anterior neurocranium and pterygoid process, in the upper jaw, migrate to condense onto the stomodeal roof. Via genetic mosaic analyses, we next show that the ventral presumptive brain is the crucial source of Hh and that stomodeal ectoderm, not the neural crest cells, is the crucial recipient of the Hh signal. Moreover, cyclopamine treatment shows that Hh acts at the end of gastrulation, substantially before crest cells migrate into the pharyngeal arches. Therefore, we conclude that Hh has a specific early role in establishing the local epithelial environment that promotes the development of the anterior craniofacial skeletal elements.

Institute of Neuroscience, 1254 University of Oregon, Eugene, OR 97403-1254, USA.

*Author for correspondence (e-mail: eberhart@uoneuro.uoregon.edu)

Accepted 11 January 2006

MATERIALS AND METHODS

Zebrafish embryos

Embryo care has been described previously (Westerfield, 1993). *fli1*:GFP transgenic embryos express GFP in cartilage-producing cells as well as vasculature (Lawson and Weinstein, 2002). Heterozygous carriers of the hypomorphic *shh* allele *syu*^{tq252} and the *smoothened* null allele *smu*^{b577} were maintained in both AB and *fli1*:GFP backgrounds and will be referred to as *shh*$^{-}$ and *smo*$^{-}$ throughout the text for clarity. *gsc*:GFP transgenic zebrafish were generated by inserting a PCR generated 3 kb 5′ upstream promoter region of the *gsc* gene, primers GC64 (5′ AGGACTACCAAGCTTACTT-TCTAACAATGCAAAGC 3′) and GC66 (5′ TAGGACGAGGGATCCC-ATCACAAGCGAAAAGATGTG 3′), into pG1 (gift of Chi-Bin Chien) and injecting early one-cell embryos with 160 ng/μl linearized plasmid. Cyclopamine treatments (Hirsinger et al., 2004) were performed on *fli1*:GFP transgenic embryos. Shh and Twhh morpholinos are described elsewhere (Nasevicius and Ekker, 2000).

Cellular analyses

colIIa (Yan et al., 1995), *fgf8* (Reifers et al., 1998), *pitx2* (Essner et al., 2000), *shh* (Krauss et al., 1993) and *sox9a* (Cresko et al., 2003) probes were used for in situ hybridization (Westerfield, 1993). For cartilage and bone staining, 4 day postfertilization (dpf) zebrafish embryos were stained with Alcian Blue and flat mounted (Kimmel et al., 1998). Time-lapse recordings, 10-15 minutes/frame, and confocal analysis of *fli1*:GFP and *smo*$^{-}$*;fli1*:GFP embryos were performed according to established protocols (Crump et al., 2004a).

Fate mapping and microelectroporation

Fate-map analyses with Kaede (Ando et al., 2002) and microelectroporation (Crump et al., 2004b) were performed in *albino;fli1*:GFP or *albino;fli1*:GFP; *h2a*:GFP transgenic embryos to allow for specific visualization of neural crest cells and chondrocytes. *Kaede* mRNA was injected at the one-cell stage. Green to red photoconversion of Kaede in a three- to five-cell diameter column was achieved using a DAPI filter set and a 30 μm pinhole. Embryos were imaged using a Zeiss Pascal confocal microscope and LSM software immediately post-labeling and again at 4.5 to 5 dpf. The original and skeletal locations of labeled cells were compiled into a fate map using the eye, the ventral limit of the crest population and the curvature of the yolk as landmarks at 12 hpf and the eye, stomodeum and first pharyngeal pouch as landmarks at 24 hpf. Statistical analysis was performed using JMP software (SAS Institute, Cary, NC).

Cell transplants

Genetic mosaics were generated as described elsewhere (Crump et al., 2004a; Maves et al., 2002). Transplants placed just to the future ventral side of the animal pole contribute to stomodeal ectoderm (Fig. 7C). Transplanting *gsc*:GFP-positive cells into the *gsc*:GFP-positive region of host embryos at 30% epiboly targeted axial mesoderm. An anterior craniofacial 'skeletal index' was used to quantify the level of rescue in *shh* + *twhh* MO-injected embryos: 0, no anterior neurocranium or pterygoid process; 1, anterior neurocranium: a very short midline bar, no pterygoid process; 2, anterior neurocranium: a longer midline bar extending between the eyes, pterygoid process present; 3, anterior neurocranium with bilateral trabeculae and slightly truncated ethmoid plate, pterygoid process present; 4, wild type.

RESULTS

Hh is required for development of the anterior craniofacial skeleton

Brand et al. described a phenotypic series of zebrafish 'midline' mutants in which cartilages of the anterior region of the skull base, or neurocranium, are increasingly reduced or lost (Brand et al., 1996; Kimmel et al., 2001). Subsequent identification of the mutated genes, e.g. *gli1* and *gli2*, showed that all of them are in the Hh pathway (Karlstrom et al., 1999; Wolff et al., 2004). We observe that hypomorphic *shh* mutant larvae display the entire phenotypic series reported by Brand et al. In the most severe hypomorphs, the anterior region of the neurocranium, including the midline ethmoid plate and the bilateral pair of trabeculae, is entirely absent. The more posterior neurocranium is only relatively mildly reduced (Fig. 1A,B). The boundary between the anterior deleted and posterior nondeleted regions is where the trabeculae meet the basal plate ('polar cartilage' region) (Cubbage and Mabee, 1996; Schilling and Kimmel, 1997). Although not reported previously, we also discovered that a specific anterior region of the palatoquadrate cartilage, the pterygoid process, was also missing in severely affected *shh* hypomorphs (Fig. 1B). The pterygoid process articulates with the ethmoid, thus connecting the jaw skeleton to the neurocranium and acting as the upper jaw cartilage (DeBeer, 1937). Additionally, the posterior portions of the palatoquadrates fuse into a single element bridging the midline. Whereas partial loss of Hh signaling predominantly affects anterior craniofacial cartilages, more complete reduction of the pathway, in severe *smo* loss-of-function mutants (Chen et al., 2001), deletes nearly all cartilage (Fig. 1C).

From these findings, we hypothesized that Hh signaling plays at least two roles. One function, revealed in the hypomorphic *shh* mutant and examined in detail here, is to pattern the formation of the anterior craniofacial skeleton specifically. A second function, revealed in the *smo* mutant, would direct differentiation of nearly all cartilages later (Long et al., 2003; Long et al., 2001). This hypothesis predicts that *smo* mutants would display early specific defects, even

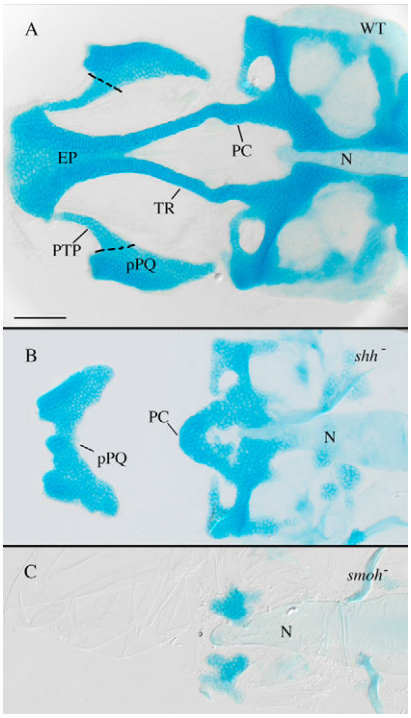

Fig. 1. Anterior craniofacial cartilages are especially sensitive to loss of Hh signaling. (**A**) Flat-mounted 4 dpf wild-type anterior craniofacial cartilages. The anterior neurocranium consists of the trabeculae (TR) and the ethmoid plate (EP). The polar cartilages (PC) fuse with TR joining the anterior and more posterior neurocranium. The dorsal first arch cartilage palatoquadrate (pPQ) and its pterygoid process (PTP) are flat mounted with the neurocranium. (**B**) Hypomorphic *shh*$^{-}$ embryos have variable anterior neurocranium defects, including loss of anterior neurocranium and PTP with fusion of pPQ across the midline. (**C**) Loss of Hh signaling in *smo*$^{-}$ embryos eliminates most neurocranium cartilages obscuring analysis of defects specific to the anterior neurocranium. N, notochord; WT, wild type. Dorsal views, anterior is leftwards in all panels. Scale bar: 50 μm.

though specific cartilage loss is not observed later due to the generalized cartilage deficiency. To look for early patterning defects in *smo* mutants, we examined the expression of two of the earliest chondrogenic markers, *sox9a* (Fig. 2) and *collIa* (data not shown). Both markers prefigure the wild-type neurocranium at 2 dpf. However, anterior neurocranial expression is completely missing in *smo* mutants, while posterior neurocranial expression remains. Hence, as predicted, we see an early *smo*$^{-}$ patterning defect that correlates with the *shh*$^{-}$ skeletal defect, even though these defects are obscured in older *smo* mutants owing to the generalized cartilage loss.

The anterior craniofacial skeleton derives from neural crest cells that condense on stomodeal ectoderm

To understand the early role of Hh signaling in development of the anterior-most head skeleton we need a detailed knowledge of how this region develops. Pharyngeal cartilages originate from neural crest cells in zebrafish as in other vertebrates (Köntges and Lumsden, 1996; Langille and Hall, 1988; Sadaghiani and Thiebaud, 1987; Schilling and Kimmel, 1994; Tan and Morriss-Kay, 1986). We now show that the zebrafish anterior neurocranium is also neural crest derived (see also Wada et al., 2005). We used

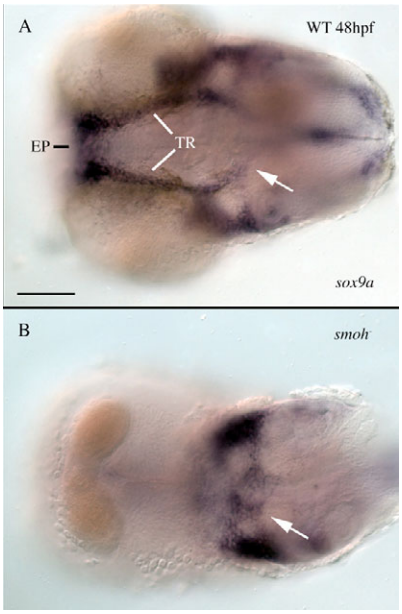

Fig. 2. *smo*⁻ mutant embryos have no anterior neurocranium precartilage condensations. Embryos were stained with RNA probe to the precartilage marker *sox9a*, the pharyngeal arches were dissected away from the embryos and ventral views of the neurocranium were imaged. (**A**) At 48 hpf, *sox9a*-positive cells prefigure the morphology of the 4 dpf neurocranium in wild-type embryos. (**B**) Embryos lacking all Hh signaling have a complete loss of anterior neurocranium precartilage condensations; however, immediately posterior precartilage condensations are present (arrows in A,B). EP, ethmoid plate; TR, trabeculae; WT, wild type. Anterior is leftwards. Scale bar: 50 μm.

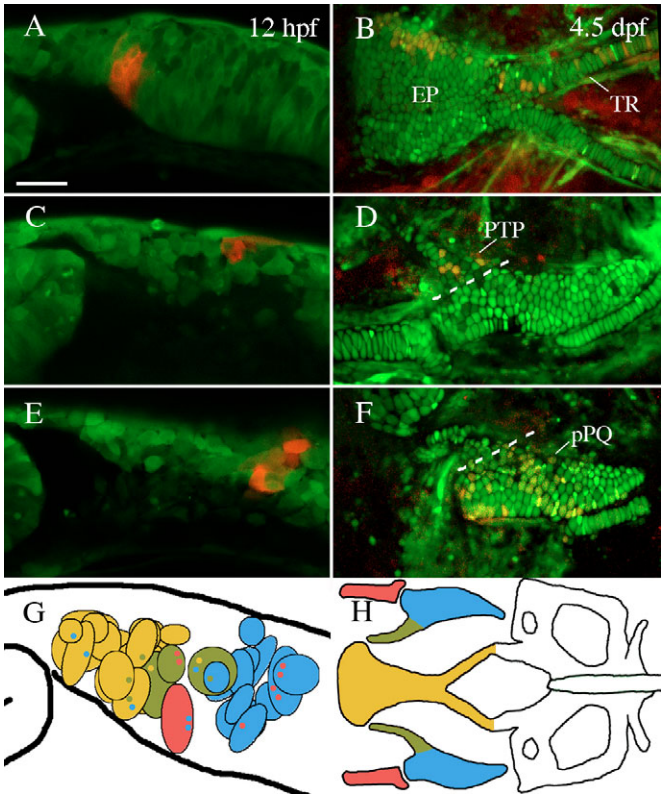

Fig. 3. The anterior neurocranium of zebrafish is neural crest-derived. (A,C,E) Lateral views of premigratory crest labeled via photoconversion of Kaede at 12 hpf. (B,D,F) Embryos reimaged at 4.5-5 dpf. (**A**,**B**) Cells labeled just posterior to the eye contributed to the ethmoid plate (EP) and trabeculae (TR). (**C**,**D**) Neural crest cells slightly more posterior contributed to pterygoid process of the palatoquadrate (PTP). (**E**,**F**) Premigratory non-pterygoid palatoquadrate (pPQ) precursors were the most posteriorly localized first arch derivative. (**G**,**H**) Schematic representations of fate mapping results show an anteroposterior bias in first arch cartilage elements. Premigratory anterior neurocranium (*n*=18) and pterygoid process (*n*=3) precursors (yellow and olive, respectively) are localized more anteriorly than Meckel's cartilage (MC) (*n*=1) and palatoquadrate (*n*=11) precursors (red and blue, respectively). Black outlined circles represent individual labeled embryos. Small colored dots within a field represent secondary cartilage fates from the field of cells. (A,C-G) Lateral views. (B,H) Dorsal views. Anterior is leftwards in all panels. Scale bar: 50 μm.

photoconversion of Kaede protein to fate map small clusters of cells in the premigratory anterior cranial neural crest, resulting in labeling in descendant chondrocytes of the trabeculae and ethmoid cartilages (Fig. 3). We also confirmed (Schilling and Kimmel, 1994) that the palatoquadrate and Meckel's cartilage derive from this population. However, labeling never included the polar cartilages or basal plate, consistent with the proposed mesodermal origin of these more posterior cartilages (Couly et al., 1993; Huang et al., 1997).

The fates of specific skeletal elements might be nonrandomly distributed within the premigratory crest, in spite of overlaps being present. The more anterior crest cells preferentially contribute to the anterior neurocranium (Fig. 3A,B), and the more posterior cells contribute to the first arch pharyngeal skeleton (Meckel's cartilage and posterior palatoquadrate; Fig. 3E,F). Notably, the pterygoid process of the palatoquadrate maps largely in between these two regions (Fig. 3C,D), in fact more frequently overlapping with neurocranial fates than with the posterior palatoquadrate (Fig. 3G,H).

We examined fates of the more anterior region at higher resolution by marking single crest cells (occasionally neighboring cell pairs) by microelectroporation before (Fig. 4A) or after (Fig. 4E) migration to the first pharyngeal arch. This method shows the precursors for the pterygoid process and anterior neurocranial cartilages, and the dermal parasphenoid bone to be largely localized to a small region along the side of the neural keel and just posterior to the rudiment of the eye (Fig. 4, data not shown). The premigratory domain is largely surrounded by crest cells that contribute, in part, to non-skeletal tissues such as the sclera of the eye.

This study also reveals that after migration, the neural crest-derived cells generating the skeletal fates described above all populate the first pharyngeal arch. Here, those cells forming specifically the pterygoid process and anterior neurocranium reside within a compact condensation closely associated with invaginated oral, or stomodeal ectoderm. Furthermore, the cells in question occupy just the part of the condensation that is present on the roof of the stomodeal epithelium (Fig. 4E-H, the extent of the domain is demarcated by the broken line in Fig. 4F). In addition, we labeled maxillary osteocytes from precursors within this domain in two cases (data not shown). Fate mapping of postmigratory posterior palatoquadrate and Meckel's cartilage precursors within the first arch is described elsewhere (J.G.C., M.E.S., J.K.E. and C.B.K., unpublished). In summary, we show that the cartilages that have an early and sensitive requirement for Hh signaling also have a distinctive origin in the neural crest, both before and after crest cells migrate to the first pharyngeal arch.

Condensation of a subset of first arch crest cells and stomodeal ectoderm marker expression is dependent on Smo function

What is the effect of reduced Hh signaling on early development of the crest-derived anterior craniofacial precursors? We observed no changes in crest cell migration between wild types and *smo* mutants, either by examining expression of a crest cell marker, *sox9b* (12 and 18 hpf, data not shown) or by Kaede labeling of premigratory neural crest cells (see Fig. S1 in the supplementary material). However, we found that postmigratory *smo*$^{-}$ cells in the first arch fail to undergo condensation on the roof of the stomodeum. To show this defect directly, we made confocal time-lapse recordings and followed cells expressing the *fli1*:GFP transgene, which labels crest cells beginning shortly after their migration and throughout skeletogenesis. At 20 hpf, postmigratory neural crest cells distribute in a broad anteroposterior swath in the first arch of wild-type and *smo*$^{-}$ embryos alike (Fig. 5A,E).

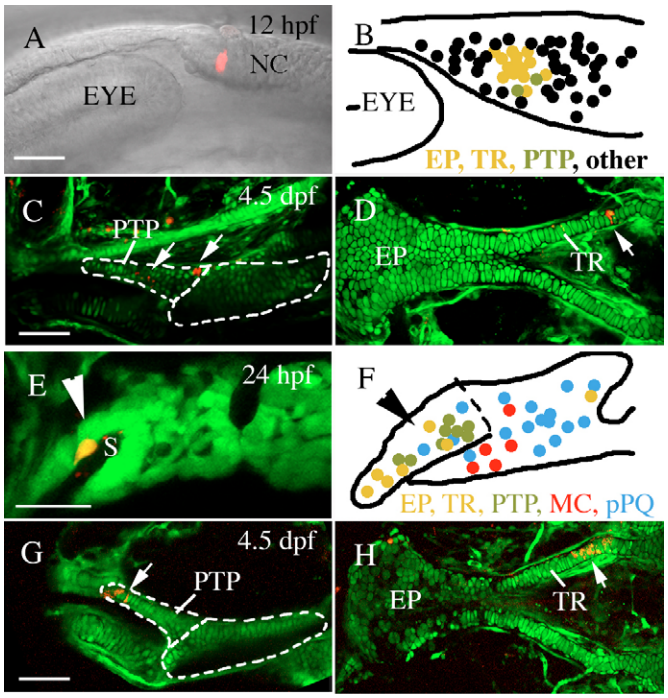

Fig. 4. Pre- and postmigratory anterior neurocranium and upper jaw precursors co-localize. Single or two adjacent neural crest cells were labeled via microelectroporation at 12 hpf (A-D) or 24 hpf (E-H, Meckel's cartilage and palatoquadrate data reanalyzed from Crump et al. unpublished). (**A-D**) At 12 hpf, pterygoid process (C, arrows, *n*=2) and anterior neurocranium (D, arrow, *n*=14) precursors are localized to a discrete cluster postoptically (B). (**E-H**) Within the first arch, at 24 hpf, pterygoid process (G, arrow, *n*=8) and anterior neurocranium (H, arrow, *n*=7) progenitors co-mingle on the stomodeal roof, away from Meckel's cartilage (*n*=5) and palatoquadrate (*n*=16) precursors. The condensed anterior craniofacial neural crest precursor domain is indicated by arrowheads in E and F. (B,F) Schematic enlargements of A and E showing compiled fate mapping data for 12 hpf (B) and 24 hpf (F). Anterior neurocranium, yellow; pterygoid process, olive; non-pterygoid palatoquadrate, blue; Meckel's cartilage, red. Black dots in B represent fates other than 4.5 dpf skeletal elements. EP, ethmoid plate; MC, Meckel's cartilage; NC, neural crest; pPQ, non-pterygoid palatoquadrate; PTP, pterygoid process of the palatoquadrate; TR, trabeculae. Anterior is leftwards in all panels. (A,B,D-F,H) Dorsal is upwards. (C,G) Dorsal views. Scale bar: 50 μm.

Similarly, in both wild type and *smo*$^{-}$, the inpocketed stomodeal ectoderm upon which the crest cells normally condense becomes evident at 21 hpf as an unlabeled (dark) indentation of the GFP-expressing cell mesenchyme (Fig. 5B,F, arrowhead). Beginning at 22 hpf, the wild-type crest cells form a prominent condensation, coating both the stomodeal roof and floor, i.e. the superior and inferior surfaces (Fig. 5C,D, see Movie 1 in the supplementary material). By contrast, in *smo* mutant embryos, neural crest cells condense only poorly or not at all on the stomodeal roof, whereas cells condense seemingly normally on the floor of the stomodeum (Fig. 5G,H, see Movie 2 in the supplementary material). Thus, the selective requirement for *smo*$^{+}$ in the condensation of crest cells on the stomodeal roof, but not floor, corresponds exactly to the selective loss of the anterior neurocranium and pterygoid process cartilages that we fate mapped to this superior region of the condensation. By 30 hpf, we could detect few, if any, crest cells condensed on the roof of the stomodeum in *smo*$^{-}$ embryos (see below, Fig. 7B). Time lapse analyses of *smo*$^{-}$ embryos from 22-48 hpf show that the mesenchymal cells that would normally condense tightly on the roof of the stomodeum instead remained loosely associated with one another and eventually migrated immediately posterior to the eye (see Movie 3 in the supplementary material). In addition, we detect no cell death in these neural crest cells even as late as 60 hpf (Acridine Orange labeling, data not shown), suggesting that Hh signaling is necessary for the condensation but not survival of this subpopulation of first arch neural crest cells.

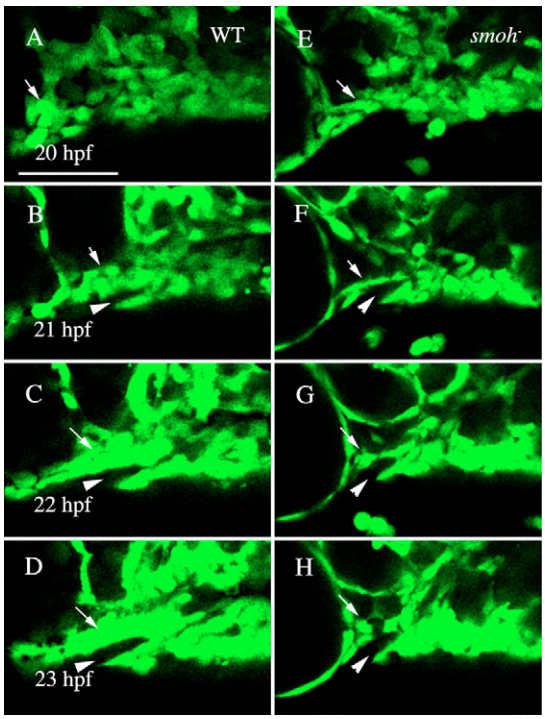

Fig. 5. Neural crest cells fail to condense upon the stomodeal roof in *smo*$^{-}$ embryos. (**A-D**) Wild-type *fli1*:GFP embryo. Movie frames are shown every hour from 20 to 23 hpf. Wild-type crest cells are condensing on the stomodeum by 22 hpf (C, arrow) and by 23 hpf (D, arrow) a solid mass surrounding the stomodeum (arrowhead) has formed. (**E-H**) Neural crest cell behavior in *smo*$^{-}$ embryos. Crest cells are present just posterior to the eye in *smo*$^{-}$;*fli1*:GFP at 20 hpf (E, arrow). However, these cells fail to condense on the roof of the stomodeum (F-H, arrow). Lateral views, dorsal is upwards. WT, wild type. Scale bar: 50 μm.

The association of the crest-derived mesenchyme with the superior surface of the stomodeal ectoderm, intimate in the wild type and missing in the *smo* mutant, prompted us to look, using marker expression, for defects in the *smo*⁻ stomodeum that could indicate a missing crucial epithelial-mesenchymal interaction (Crump et al., 2004b; Hall, 1992). *pitx2* (expressed broadly in wild type, Fig. 6A), *fgf8* (lateral stomodeum, Fig. 6C) and *shh* (medial stomodeum, Fig. 6E) are all strikingly downregulated in the *smo*⁻ stomodeum (Fig. 6B,D,F). Some *shh*-expressing cells, probably endodermal but possibly stomodeal, are still present in the mutant near the midline (Fig. 6F, see Fig. S2 in the supplementary material). The stomodeum is not simply missing in *smo* mutants; we can detect it by morphology with DIC optics and it expresses epithelial markers (see Fig. S3 in the supplementary material, data not shown). Moreover, we detected no cell death by Acridine Orange staining, loss of proliferation by anti-phosphohistone H3 or alterations of the early gastrula fate map of the stomodeum in *smo*⁻ embryos (data not shown).

Reception of Hh signaling is required in the stomodeal ectoderm, not neural crest cells, for condensation of crest cells on the stomodeal roof

Smo-dependent gene expression points to the stomodeal ectoderm as a potential direct target of Hh signaling, in which case the disruption of condensation of the crest-derived mesenchyme in *smo* mutants could be indirect. However, the opposite interpretation is also possible: work in mouse has shown that reception of Hh signaling is required by neural crest cells for craniofacial development (Jeong et al., 2004), and neural crest cells have been shown to regulate the timing of gene expression in avian facial ectoderm (Schneider and Helms, 2003). To determine which tissue needs to receive Hh signaling to promote crest cell condensation, we used mosaic analysis with wild-type and *smo*⁻ embryos. In wild-type hosts that received transplants of *smo*⁻ crest cell precursors, *smo*⁻ crest cells condensed apparently normally on the stomodeal roof (Fig. 7A,C). This rescue suggests that Smo functions nonautonomously in crest condensation. However, we rarely

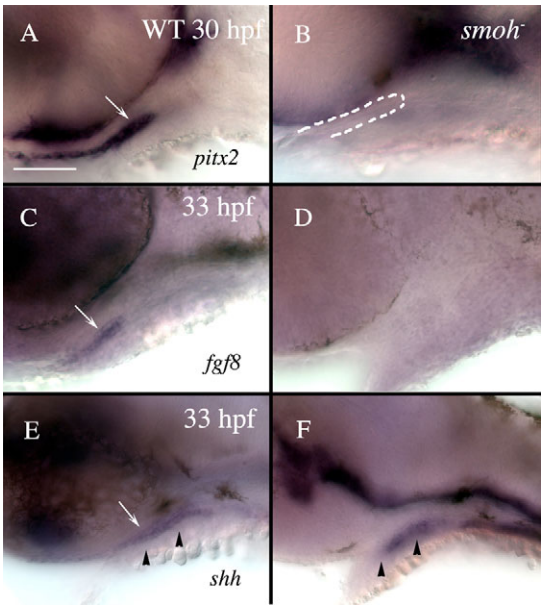

Fig. 6. Loss of Hh function causes loss of stomodeum specification. Lateral views of 30 hpf (A,B) or 33 hpf (C-F) wild-type (A,C,E) or *smo*⁻ (B,D,F) embryos labeled with RNA probe to *pitx2* (A,B), *fgf8* (C,D) or *shh* (E,F). (**A**) Wild-type embryos strongly express *pitx2* throughout the stomodeum (arrow), while (**B**) *smo*⁻ embryos have no detectable *pitx2* expression in the stomodeum, although a morphologically identifiable stomodeum is present (outlined in B). (**C**) *fgf8* labels the lateral stomodeum in wild-type embryos (arrow). (**D**) No *fgf8* expression is detectable in the stomodeum of *smo*⁻ embryos. (**E**) *shh* labels wild-type medial stomodeum (arrow). (**F**) However, *shh* is not evident in the stomodeum of *smo*⁻ embryos, although some medial cells, presumably endoderm, maintain *shh* expression. Arrowheads in E and F indicate the level of sections shown in Fig. S3. Dorsal is upwards. WT, wild type. Scale bar: 50 μm.

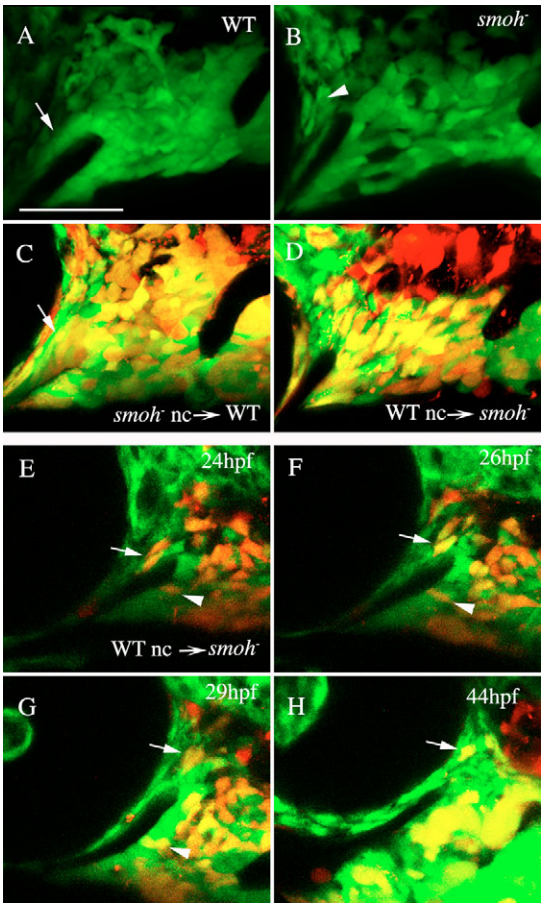

Fig. 7. Reception of Hh signaling is not required in neural crest cells to condense on the stomodeum. (**A**) A tight neural crest cell condensation coats the stomodeum in wild-type 30 hpf *fli1*:GFP embryos (arrow). (**B**) The region of this condensation superior to the stomodeum is absent in *smo*⁻;*fli1*:GFP embryos, although GFP-positive sclera is present surrounding the eye (arrowhead). (C,D) 30 hpf embryos following transplantation between wild-type and *smo*⁻ embryos. (**C**) *smo*⁻ neural crest cells readily condense on the stomodeal roof in wild-type embryos (arrow, *n*=12). (**D**) Crest cells from wild-type donors fail to condense on the stomodeal roof in *smo*⁻ embryos, even though they can populate the region occupied by palatoquadrate and Meckel's cartilage precursors (*n*=18). (**E-H**) Images taken from a time-lapse recording (*n*=2) of wild-type crest in a *smo*⁻ host. Wild-type neural crest cells are capable of initially populating the region superior to the stomodeum (E-H, arrow); however, these cells are not stabilized in this position and eventually migrate posterior to the eye. Wild-type cells in the Meckel's cartilage domain condense normally (E-G, arrowhead). Lateral views, dorsal is upwards. nc, neural crest; WT, wild type. Scale bar: 50 μm.

observed *smo*⁻ cells in cartilages at 4 dpf in these mosaics (data not shown), consistent with a later autonomous Smo-dependency in crest for cartilage differentiation (as also reported recently by Wada et al., 2005). In the reciprocal experiment, wild-type crest when transplanted into *smo*⁻ hosts failed to condense on the stomodeal roof, just as in *smo* mutants (Fig. 7B,D), and again suggesting that the Smo requirement for condensation is crest nonautonomous. Furthermore, time-lapse analyses of mosaics directly show that wild-type crest cells in the *smo*⁻ environment enter the region superior to the stomodeum (Fig. 7E) but they fail to condense (Fig. 7F-H, see Movie 4 in the supplementary material), just as described for the *smo* mutants themselves (Fig. 5).

These experiments show that Smo function is not directly required in neural crest cells for condensation. Hence, we used mosaic analysis to examine the other possibility, that the stomodeum itself is the target of Hh signaling. By transplanting the rudiment of the stomodeum, we generated mosaic embryos in which wild-type donor cells contributed to the stomodeum in *smo*⁻ hosts. In these mosaics, the *smo*⁻ crest cells condensed on the transplanted wild-type stomodeum normally, and also correctly expressed the chondrogenic marker *sox9a* (Fig. 8C,D). Rescue of both the condensation and *sox9a* expression was unilateral in the mosaics, corresponding to the side that received the wild-type stomodeal transplant (Fig. 8D,E). Sometimes the transplants included non-stomodeal facial ectoderm. However, stomodeal ectoderm was the only tissue that always correlated with rescue, suggesting that the response to Hh signaling is required directly within the stomodeal precursors. A robust condensation on the stomodeal roof persists for at least 1 day in the mosaics (through at least 48 hpf; see Fig. S4 in the supplementary material). However, no cartilage develops, which is consistent, as argued above, with a later direct requirement for Smo function in the crest-derived skeletogenic cells. Again, the result indicates the occurrence of a later Hh-signaling event required for skeletogenesis, one separate from the early signaling for condensation.

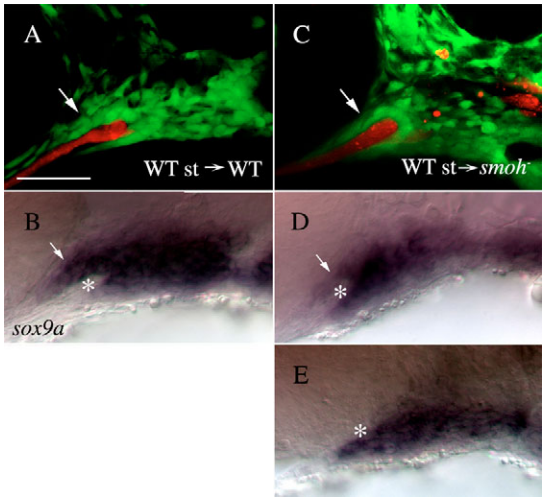

Fig. 8. Wild-type stomodeum rescues the condensation of anterior craniofacial neural crest cells in *smo*⁻ embryos. (A,C) Lateral views of *fli1*:GFP (A) or *smo*⁻;*fli1*:GFP (C) embryos at 30 hpf following transplantation of wild-type stomodeum. (**A**) Neural crest cells condense on the stomodeal roof following control transplants (arrow). (**C**) Following transplantation of wild-type stomodeum into *smo*⁻, crest cells condense on the roof of the stomodeum, in a manner similar to that seen in wild type (arrow, *n*=9). (B,D,E) Lateral views of the same embryos in A,C labeled with RNA probe to *sox9a*. (**B**) sox9a-positive cells (arrow) are clearly visible above the stomodeum (*) in control transplanted embryos. (**D**) *sox9a*-expressing neural crest cells (arrow) are readily apparent superior to the stomodeum (*) on the side of the embryo receiving the stomodeal transplant. (**E**) Control, non-transplanted, side of the same embryo as B (image flipped to be the same orientation as that in D). No sox9a-positive cells are observed above the stomodeum (*). Anterior is leftwards. st, stomodeum; WT, wild type. Scale bar: 50 μm.

Hh signaling for anterior craniofacial crest cell condensation is required at the end of gastrulation from the rudiment of the ventral brain

Our mosaic analyses provide direct evidence that the reception of Hh signaling is required in the stomodeal ectoderm for the condensation of crest cells upon its roof. When does signaling to the stomodeum occur and what is the signaling source? To address the first part of this question, we used timed treatments with cyclopamine to disrupt the Hh pathway at specific stages and assayed the effects. We found that 4 hours of cyclopamine exposure,

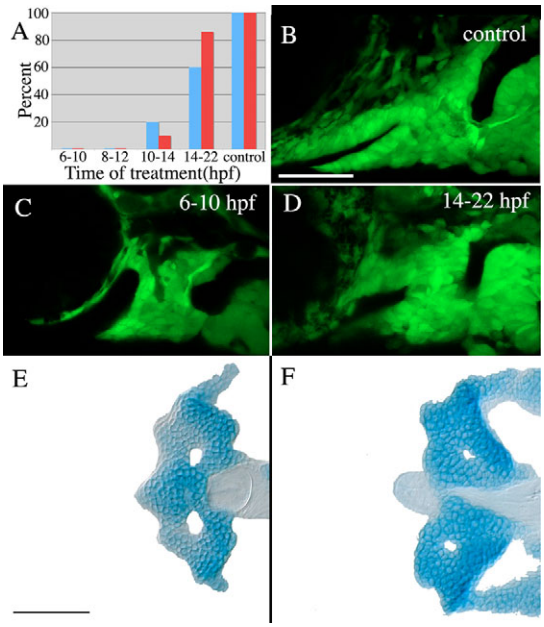

Fig. 9. Hh signaling is required at the end of gastrulation for stomodeum expression of *pitx2* and proper crest cell condensation. (**A**) No embryos treated with cyclopamine from 6-10 hpf or 8-12 hpf express stomodeal *pitx2* (blue bars) or condense crest on the stomodeal roof (red bars). A small number of embryos treated with cyclopamine from 10-14 hpf express *pitx2* in the stomodeum and exhibit condensation of anterior craniofacial crest cells, whereas the majority of embryos treated between 14-22 hpf do express *pitx2* in the stomodeum and condense crest cells on the roof of the stomodeum. Control DMSO-treated embryos all expressed *pitx2* and undergo crest cell condensation normally. (**B-D**) Effects of cyclopamine treatment on the condensation of neural crest cells. Anterior craniofacial crest cells condense on the stomodeal roof in control embryos (B) and embryos treated from 14-22 hpf (D); however, this crest cell subpopulation fails to condense in embryos treated from 6-10 hpf (C). (**E**,**F**) The anterior neurocranium is deleted in all cyclopamine-treated embryos. *n*=10 in each treatment group for *pitx2* expression. Crest cell condensation and neurocranial cartilage analysis: 6-10 hpf, *n*=25; 8-12 hpf, *n*=16; 10-14 hpf, *n*=20; 14-22 hpf, *n*=21; control, *n*=14. Scale bars: 50 μm.

if initiated at 8-12 hpf or earlier, completely eliminated both stomodeal *pitx2* expression and crest cell condensation on the stomodeal roof (Fig. 9A,C). Later treatments, even if longer in duration, were less effective by these assays (e.g. an 8 hour treatment from 14-22 hpf; Fig. 9A,D). Consistent with previous findings (Hirsinger et al., 2004), we found *ptc1* levels to be highly disrupted 1 hour after cyclopamine treatment begins (data not shown). Therefore, the crucial time for Hh signaling to correctly specify marker expression in the stomodeum is about 10 hpf, shortly after gastrulation. Continued Hh signaling after 10 hpf is also likely to be important (Fig. 9A). Regardless of timing, all cyclopamine treatments resulted in severe pharyngeal cartilage loss that included first arch palatoquadrate and Meckel's cartilages (data not shown). Additionally, all cyclopamine treated embryos lacked the anterior neurocranium (Fig. 9E,F). However, as crest cells condense on the stomodeal roof in later treated embryos, the subsequent loss of the anterior neurocranium is probably due to the cell-autonomous requirement for Hh signaling as described for the mosaic analyses. Indeed, *ptc1*, a Hh signaling readout gene, is not expressed by neural crest cells at 14 hpf, but can be detected in neural crest cells adjacent to the eye at 22 hpf (data not shown).

At 10 hpf, the crucial time when the stomodeum must receive Hh signaling, the only Hh sources present in the head rudiment are Shh and its co-ortholog Twhh. Specifically, both are expressed in the midline by the ventral neural keel and the prechordal plate (Ekker et al., 1995; Krauss et al., 1993). Here, we use Hh-deficient mosaics to test which tissue is the crucial source of the Hh signal. To create animals deficient for both Shh and Twhh, we co-injected two morpholinos that individually block translation of *shh* or *twhh* (*shh*-MO; *twhh*-MO). The double morpholino treatment consistently resulted in the loss of crest cell condensation on the stomodeal roof (Fig. 10A) and a resulting loss of the anterior craniofacial skeleton, similar to the most severe *shh* hypomorphic mutants (Fig. 10; compare D and E with Fig. 1A and B, see legend for quantification). The stomodeal expression of *pitx2*, *shh* and *fgf8* in *shh*-MO; *twhh*-MO embryos was greatly diminished (data not shown), although less consistently than in *smo* mutants. Transplantation of wild-type presumptive ventral midbrain into *shh*-MO; *twhh*-MO hosts was able to significantly rescue both condensation and skeletal phenotypes (Fig. 10B,F), and the level of rescue positively correlated with the number of donor cells populating the ventral brain (data not shown). By contrast, even in instances when donor cells extensively populated the prechordal plate and notochord, the embryos still developed virtually no anterior craniofacial skeleton (Fig. 10C,G). Therefore, only the ventral brain is a significant Hh source for promoting condensation of crest cells on the stomodeal roof.

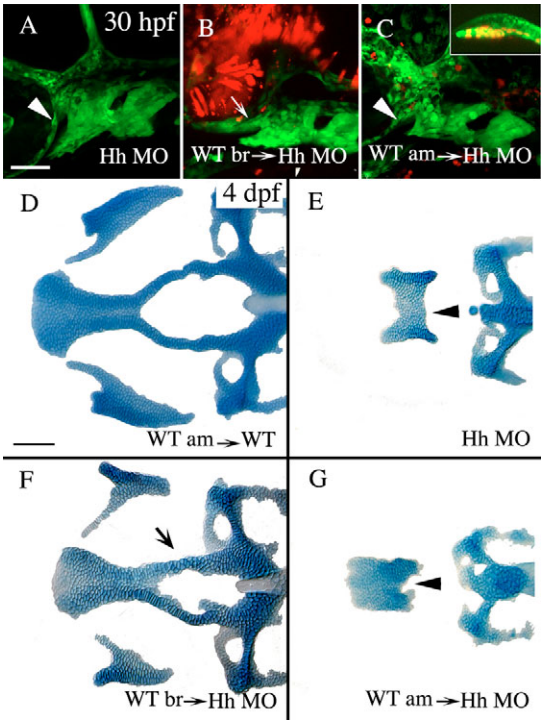

Fig. 10. Hh secreted from the ventral presumptive brain, and not the axial mesoderm, is required for condensation of crest cells on the roof of the stomodeum and the subsequent formation of the anterior craniofacial skeleton. (**A-C**) Lateral views of 30 hpf *fli1*:GFP embryos co-injected with *shh* and *twhh* morpholinos (Hh MO). (**D-G**) Dorsal views of Alcian stained 4 dpf neurocrania and palatoquadrates from control transplanted embryos (D) or embryos co-injected with Hh MO (E-G). (A,E) Co-injection of Hh MO causes failure of crest cells to condense on the stomodeal roof (A, arrowhead) and the development of the derivatives from this region, the anterior neurocranium and pterygoid process (E, arrowhead; skeletal index=0.1, *n*=57). (B,F) Transplantation of wild-type brain into Hh MO-injected embryos is capable of rescuing the condensation of neural crest cells (B, arrow) and the skeletal derivatives almost to wild-type morphology (F, arrow, skeletal index=2.2, *n*=40, ANOVA F ratio=64.481, *P*<0.0001, Tukey-Kramer shows significance is only attributable to wild-type brain transplant). (C,G) Transplantation of axial mesoderm, including prechordal plate (C, inset), into Hh MO injected embryos has no effect on crest cell condensation (C, arrowhead) or on anterior neurocranium and upper jaw cartilage morphology (G, arrowhead, skeletal index=0.2, *n*=14). Anterior is leftwards. am, axial mesoderm; br, brain; WT, wild type. Scale bar: 50 μm.

DISCUSSION

At the end of gastrulation, Hh secreted from the ventral brain primordium signals to ectodermal precursors of the stomodeum (Fig. 11A). Hh signaling specifies a relay, the ability of the stomodeum to interact with cranial neural crest cells that arrive in the vicinity some 8 to 10 hours later (Fig. 11B). The relaying signal from the stomodeum clearly does not involve Hh, probably occurs at close range, and is required for the condensation of neural crest cells upon the stomodeal roof. These condensed cells will generate the anterior craniofacial skeleton – the pterygoid process of the palatoquadrate in the upper jaw and the anterior neurocranium.

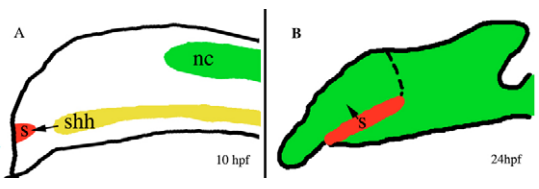

Fig. 11. Hh signaling specifies the ability of the stomodeum to condense neural crest cells on its roof. (**A**) Schematic of a 10 hpf embryo. Shh (yellow) secreted from the ventral presumptive brain signals to stomodeum precursors (red) in the anterior ectoderm. Premigratory neural crest cells (green) are distant from the Hh source. (**B**) Later in development, starting at 21 hpf, the stomodeum signals to neural crest cells through an unknown mechanism, causing anterior craniofacial neural crest cells to condense.

Furthermore, it is clear that for proper craniofacial development multiple reciprocal signaling interactions must continue after this early Hh-mediated signal and its relay, that we characterize in this paper. The recent work of Wada et al. (Wada et al., 2005), supported by our own study, clarifies that in zebrafish there occurs another, later signaling interaction that redeploys Hh, probably now secreted by oral ectoderm and acting directly on the neural crest. The second Hh signal requires the first (Fig. 6). Furthermore, specifying the expression of Shh in the stomodeum appears to require signaling to the ectoderm from the neural crest (Marcucio et al., 2005).

An early role for Hh signaling in development of the anterior craniofacial skeleton

The hypothesis just described, particularly the understanding that Hh functions in two separate interactions, can resolve seemingly contradictory findings in zebrafish, chicken and mouse. Defects in the distribution of neural crest cells have been demonstrated in *Shh*-null mice (Washington et al., 2005), suggesting that the early role of Hh in organizing the condensation of crest cells on the stomodeal roof may be conserved between zebrafish and mice. In mouse mosaics, *Smo* mutant crest cells can form facial prominences in a wild-type host (Jeong et al., 2004), just as we observe *smo* mutant crest cells can develop condensations in zebrafish. Furthermore, in both species the mosaics reveal a crest-autonomous requirement for *Smo* in the formation of skeletal elements that stem from these prominences or condensations. In the chicken, early disruption of Hh signaling causes loss of expression of *Shh* and *Fgf* in facial ectoderm (Marcucio et al., 2005), matching our findings in the zebrafish, even though Marcucio et al. provide an alternative interpretation to ours, namely that the neural crest relays a Shh signal to the facial epithelium. Although our hypothesis fully explains their findings, their model could not work for zebrafish because it requires an early *smo* function in the neural crest, and we show this function is dispensable. We propose that the same early signaling cascade underlying anterior craniofacial development is widely shared among vertebrates.

The stomodeum as an organizing center for a subset of first arch crest cells

How does the stomodeum organize the condensation and later development of neural crest cells? Facial ectoderm has been shown to be important for the proper outgrowth of anterior craniofacial skeletal elements (Hu et al., 2003; MacDonald et al., 2004), and here we present data that the oral ectoderm is essential for the initial condensation of neural crest cells that contribute to these skeletal elements. The same kinds of ectomesenchymal-epithelial interactions are crucial for skeletal development in the second arch as well as the first (Crump et al., 2004a; Crump et al., 2004b). In both arches, crest cells condense on an epithelium and later chondrogenesis is strictly correlated with, and presumably dependent upon, condensation. However, in the second arch, the crucial epithelium revealed in our studies is the first pharyngeal pouch, derived from endoderm. Furthermore, we find that Hox gene expression appears to specify the ability of second arch crest cells to interact with the pouch endoderm (J.G.C., M.E.S., J.K.E. and C.B.K., unpublished). First arch crest cells lack Hox gene expression and this difference could, in part, underlie whether crest cells interact with endoderm as in the second arch, or with stomodeal ectoderm as in the first arch.

The transcription factor *pitx2* is an excellent candidate for a gene responding to Hh that regulates the role the stomodeum plays in crest cell condensation. *Pitx2* mutations in mouse and human are known to cause craniofacial defects (Lu et al., 1999; Saadi et al., 2003; Saadi et al., 2001), but it is unclear if these defects are due to the loss of *Pitx2* specifically in the stomodeum. Earlier requirements for *pitx2* in zebrafish (Essner et al., 2000) have obscured potential anterior craniofacial defects in loss-of-function analyses (J.K.E., unpublished). Conditional expression of dominant-negative *Pitx2* (Saadi et al., 2003; Saadi et al., 2001) within stomodeal ectoderm may be useful for determining the role of Pitx2 in craniofacial development in the future.

Secreted signaling factors might be involved in the stomodeal-crest cell interaction. Along with *pitx2*, both *fgf8* and *shh* are expressed by the zebrafish stomodeum (Miller et al., 2004; Miller et al., 2000) and are lost in *smo* mutants (this study). We observed little or no overlap of *shh* and *fgf8* in the wild type, and this apparent restriction may be functionally relevant because interfaces of *shh* and *fgf* expression are known to direct craniofacial outgrowth in avian embryos (Abzhanov and Tabin, 2004; Hu et al., 2003; MacDonald et al., 2004). We only detect stomodeal *shh* and *fgf8* expression after the time of crest cell condensation, arguing that their role is indeed in promoting outgrowth, rather than signaling the crest cells to condense. Although a recent study in zebrafish has reported that the stomodeum can partially rescue midline ethmoid plate defects in more mildly affected Hh mutants and *shh*-MO animals (Wada et al., 2005), we find no ability of the stomodeum to rescue the condensation and development of anterior craniofacial precursors in more severely affected *shh*-MO; *twhh*-MO embryos (data not shown).

We show that normally first arch crest cells closely adhere to both the roof and floor of the stomodeal epithelium. Our time-lapse analyses with mosaics show that wild-type crest cells in the *smo* mutant environment contact but fail to condense on the roof of the stomodeum, whereas crest cells condense normally on the mutant stomodeal floor. A clear inference is that the stomodeum provides differential adhesive substrates on the roof and floor and that Hh signaling selectively patterns the roof. Cell-ECM and cell-cell adhesion, implicated in condensing craniofacial neural crest cells (McKeown et al., 2005), may provide a mechanism for Hh mediated stabilization of anterior craniofacial neural crest cells. It will be of great interest to discover if any adhesion molecules are differentially expressed on stomodeal roof versus floor and if the expression of adhesion molecules on the roof is Hh dependent.

Supplementary material

Supplementary material for this article is available at
http://dev.biologists.org/cgi/content/full/132/6/1069/DC1

We greatly appreciate comments on the manuscript provided by R. Marcucio, C. T. Miller and T. Piotrowski. We also to thank W. A. Cresko for his statistical expertise. We are deeply indebted to J. Dowd, J. Wofford and Bonnie Ullmann for their expert fish care and technical help. We thank T. F. Schilling, N. Wada and Y. Javidan for sharing unpublished data. This work was supported by NIH grants HD22486 and DE13834 to C.B.K.; NIH Ruth L. Kirschstein NRSA HD043584 to J.K.E.; and an O'Donnell Fellowship of the Life Sciences Research Foundation to J.G.C.

References

Abzhanov, A. and Tabin, C. J. (2004). Shh and Fgf8 act synergistically to drive cartilage outgrowth during cranial development. *Dev. Biol.* **273**, 134-148.

Ando, R., Hama, H., Yamamoto-Hino, M., Mizuno, H. and Miyawaki, A. (2002). An optical marker based on the UV-induced green-to-red photoconversion of a fluorescent protein. *Proc. Natl. Acad. Sci. USA* **99**, 12651-12656.

Brand, M., Heisenberg, C.-P., Warga, R. M., Pelegri, F., Karlstrom, R. O., Beuchle, D., Picker, A., Jiang, Y.-J., Furutani-Seiki, M., van Eeden, F. J. M. et al. (1996). Mutations affecting development of the midline and general body shape during zebrafish embryogenesis. *Development* **123**, 129-142.

Chen, W., Burgess, S. and Hopkins, N. (2001). Analysis of the zebrafish

smoothened mutant reveals conserved and divergent functions of hedgehog activity. *Development* **128**, 2385-2396.
Chiang, C., Litingtun, Y., Lee, E., Young, K. E., Corden, J. L., Westphal, H. and Beachy, P. A. (1996). Cyclopia and defective axial patterning in mice lacking Sonic hedgehog gene function. *Nature* **383**, 407-413.
Cordero, D., Marcucio, R., Hu, B., Gaffield, W., Tapadia, M. and Helms, J. A. (2004). Temporal perturbations in sonic hedgehog signaling elicit the spectrum of holoprosencephaly phenotypes. *J. Clin. Invest.* **114**, 485-494.
Couly, G. F., Coltey, P. M. and LeDouarin, N. M. (1993). The triple origin of skull in higher vertebrates: a study in quail-chick chimeras. *Development* **117**, 409-429.
Cresko, W. A., Yan, Y. L., Baltrus, D. A., Amores, A., Singer, A., Rodriguez-Mari, A. and Postlethwait, J. H. (2003). Genome duplication, subfunction partitioning, and lineage divergence: Sox9 in stickleback and zebrafish. *Dev. Dyn.* **228**, 480-489.
Crump, J. G., Maves, L., Lawson, N. D., Weinstein, B. M. and Kimmel, C. B. (2004a). An essential role for Fgfs in endodermal pouch formation influences later craniofacial skeletal patterning. *Development* **131**, 5703-5716.
Crump, J. G., Swartz, M. E. and Kimmel, C. B. (2004b). An integrin-dependent role of pouch endoderm in hyoid cartilage development. *PLoS Biol.* **2**, 1432-1445.
Cubbage, C. C. and Mabee, P. M. (1996). Development of the cranium and paired fins in the zebrafish *Danio rerio* (Ostariophysi, Cyprinidae). *J. Morphol.* **229**, 121-160.
DeBeer, G. R. (1937). *The Development of the Vertebrate Skull.* Oxford, UK: Oxford University Press.
Ekker, S. C., Ungar, A. R., Greenstein, P., Kessler, D. P., Porter, J. A., Moon, R. T. and Beachy, P. A. (1995). Patterning activities of vertebrate hedgehog proteins in the developing eye and brain. *Curr. Biol.* **5**, 944-955.
Essner, J. J., Branford, W. W., Zhang, J. and Yost, H. J. (2000). Mesendoderm and left-right brain, heart and gut development are differentially regulated by pitx2 isoforms. *Development* **127**, 1081-1093.
Hall, B. K. (1992). Tissue interactions in the development and evolution of the vertebrate head. In *Evolutionary Developmental Biology* (ed. B. K. Hall), pp. 275. London, UK: Kluwer Academic.
Hirsinger, E., Stellabotte, F., Devoto, S. H. and Westerfield, M. (2004). Hedgehog signaling is required for commitment but not initial induction of slow muscle precursors. *Dev. Biol.* **275**, 143-157.
Hu, D. and Helms, J. A. (1999). The role of sonic hedgehog in normal and abnormal craniofacial morphogenesis. *Development* **126**, 4873-4884.
Hu, D., Marcucuio, R. S. and Helms, J. A. (2003). A zone of frontonasal ectoderm regulates patterning and growth in the face. *Development* **130**, 1749-1758.
Huang, R., Zhi, Q., Ordahl, C. P. and Christ, B. (1997). The fate of the first avian somite. *Anat. Embryol.* **195**, 435-449.
Jeong, J., Mao, J., Tenzen, T., Kottmann, A. H. and McMahon, A. P. (2004). Hedgehog signaling in the neural crest cells regulates the patterning and growth of facial primordia. *Genes Dev.* **18**, 937-951.
Karlstrom, R. O., Talbot, W. S. and Schief, A. F. (1999). Comparative synteny cloning of zebrafish *you-too*: mutations in the Hedgehog target *gli2* affect ventral forebrain patterning. *Genes Dev.* **13**, 388-393.
Kimmel, C. B., Miller, C. T., Kruze, G., Ullmann, B., BreMiller, R. A., Larison, K. D. and Snyder, H. C. (1998). The shaping of pharyngeal cartilages during early development of the zebrafish. *Dev. Biol.* **203**, 245-263.
Kimmel, C. B., Miller, C. T. and Moens, C. B. (2001). Specification and morphogenesis of the zebrafish larval head skeleton. *Dev. Biol.* **233**, 239-257.
Köntges, G. and Lumsden, A. (1996). Rhombencephalic neural crest segmentation is preserved throughout craniofacial ontogeny. *Development* **122**, 3229-3242.
Krauss, S., Concordet, J. P. and Ingham, P. W. (1993). A functionally conserved homolog of the *drosophila* segment polarity gene *hh* is expressed in tissues with polarizing activity in zebrafish embryos. *Cell* **75**, 1431-1444.
Langille, R. M. and Hall, B. K. (1988). Role of the neural crest in development of the cartilaginous cranial and visceral skeleton of the medaka, *Oryzias latipes* (Teleostei). *Anat. Embryol.* **177**, 297-305.
Lawson, N. and Weinstein, B. M. (2002). In vivo imiagining of embryonic vascular development using transgenic zebrafish. *Dev. Biol.* **248**, 307-318.
Long, F., Zhang, X. M., Karp, S., Yang, Y. and McMahon, A. P. (2001). Genetic manipulation of hedgehog signaling in the endochondral skeleton reveals a direct role in the regulation of chondrocyte proliferation. *Development* **128**, 5099-5108.
Long, F., Chung, U.-I., Ohba, S., McMahon, J., Kronenberg, H. M. and McMahon, A. P. (2003). Ihh signaling is directly required for the osteoblast lineage in the endochondral skeleton. *Development* **131**, 1309-1318.
Lu, M.-F., Pressman, C., Dyer, R., Johnson, R. L. and Martin, J. F. (1999). Function of Rieger syndrom gene in left-right asymmetry and craniofacial development. *Nature* **401**, 276-278.
MacDonald, M. E., Abbott, U. K. and Richman, J. M. (2004). Upper beak truncation in chicken embryos with the Cleft primary palate mutation is due to an epithelial defect in the frontonasal mass. *Dev. Dyn.* **230**, 335-349.
Marcucio, R. S., Cordero, D. R., Hu, D. and Helms, J. A. (2005). Molecular interactions coordinating the development of the forebrain and face. *Dev. Biol.* **284**, 48-61.
Maves, L., Jackman, W. and Kimmel, C. B. (2002). FGF3 and FGF8 mediate a rhombomere 4 signaling activity in the zebrafish hindbrain. *Development* **129**, 3825-3837.
McKeown, S. J., Newgreen, D. F. and Farlie, P. G. (2005). Dlx2 over-expression regulates cell adhesion and mesenchymal condensation in ectomesenchyme. *Dev. Biol.* **281**, 22-37.
Miller, C. T., Schilling, T. F., Lee, K.-H., Parker, J. and Kimmel, C. B. (2000). sucker encodes a zebrafish endothelin-1 required for ventral pharyngeal arch development. *Development* **127**, 3815-3828.
Miller, C. T., Maves, L. and Kimmel, C. B. (2004). moz regulates Hox expression and pharyngeal segment identity in zebrafish. *Development* **131**, 2443-2461.
Nasevicius, A. and Ekker, S. C. (2000). Effective targeted gene 'knockdown' in zebrafish. *Nat. Genet.* **26**, 216-220.
Reifers, F., Bohli, H., Walsh, E. C., Crossley, P. H., Stainier, D. Y. R. and Brand, M. (1998). Fgf8 is mutated in zebrafish acerebellar (ace) mutants and is required for maintenance of midbrain-hindbrain boundary development and somitogenesis. *Development* **125**, 2381-2395.
Roessler, E., Belloni, E., Gaudenz, K., Jay, P., Berta, P., Scherer, S. W., Tsui, L. C. and Muenke, M. (1996). Mutations in the human sonic hedgehog gene cause holoprosencephaly. *Nat. Genet.* **14**, 357-360.
Saadi, I., Semina, E. V., Amendt, B. A., Harris, D. J., Murphy, K. P., Murray, J. C. and Russo, A. F. (2001). Identification of a dominant negative homeodomain mutation in Rieger syndrom. *J. Biol. Chem.* **276**, 23034-23041.
Saadi, I., Kuburas, A., Engle, J. J. and Russo, A. F. (2003). Dominant negative dimerization of a mutant homeodomain protein in Axenfeld-Rieger Syndrome. *Mol. Cell. Biol.* **23**, 1968-1982.
Sadaghiani, B. and Thiebaud, C. H. (1987). Neural crest development in the *Xenopus laevis* embryo, studied by interspecific transplantation and scanning electron microscopy. *Dev. Biol.* **124**, 91-110.
Schilling, T. F. and Kimmel, C. B. (1994). Segment and cell type lineage restrictions during pharyngeal arch development in the zebrafish embryo. *Development* **120**, 483-494.
Schilling, T. F. and Kimmel, C. B. (1997). Musculoskeletal patterning in the pharyngeal segments of the zebrafish embryo. *Development* **124**, 2945-2960.
Schneider, R. A. and Helms, J. A. (2003). The cellular and molecular origins of beak morphology. *Science* **299**, 565-568.
Tan, S. S. and Morriss-Kay, G. (1986). Analysis of cranial neural crest cell migration and early fates in postimplantation rat chimaeras. *J. Embryol. Exp. Morphol.* **98**, 21-58.
Wada, N., Javidan, Y., Nelson, S., Carney, T. J., Kelsh, R. N. and Schilling, T. F. (2005). Hedgehog signaling is required for cranial neural crest morphogenesis and chondrogenesis at the midline in the zebrafish skull. *Development* **132**, 3977-3988.
Walshe, J. and Mason, I. (2003). Fgf signalling is required for formation of cartilage in the head. *Dev. Biol.* **264**, 522-536.
Washington, S. I., Byrd, N. A., Abu-Issa, R., Goddeeris, M. M., Anderson, R., Morris, J., Yamamura, K., Klingensmith, J. and Meyers, E. N. (2005). Sonic hedgehog is required for cardiac outflow tract and neural crest cell development. *Dev. Biol.* **283**, 357-372.
Westerfield, M. (1993). *The Zebrafish Book: A Guide for the Laboratory use of Zebrafish (*Brachydanio rerio*)*. Eugene, OR: University of Oregon.
Wolff, C., Roy, S., Lewis, K. E., Schauerte, H., Joerg-Rauch, G., Kirn, A., Weiler, C., Geisler, R., Haffter, P. and Ingham, P. W. (2004). *iguana* encodes a novel zinc-finger protein with coiled-coil domains essential for Hedgehog signal transduction in the zebrafish embryo. *Genes Dev.* **18**, 1565-1576.
Yan, Y. L., Hatta, K., Riggleman, B. and Postlethwait, J. H. (1995). Expression of a type II collagen gene in the zebrafish embryonic axis. *Dev. Dyn.* **203**, 363-376.